

LETTERS



Wind farm layout optimization using genetic algorithm and its application to Daegwallyeong wind farm

Jeong Woo Park¹ · Bo Sung An² · Yoon Seung Lee² · Hyunsuk Jung² · Ikjin Lee¹

Received: 15 July 2019 / Revised: 9 October 2019 / Accepted: 21 October 2019 / Published online: 13 November 2019
© The Korean Society of Mechanical Engineers 2019

Abstract

This paper proposes a new wind farm layout optimization methodology based on a genetic algorithm by implementing a simulation model considering wake effect. This method consists of (1) batch optimization to efficiently obtain a rough wind farm layout for the maximum energy production in a large scale, and (2) post-optimization to obtain a refined layout to further improve the energy production in a small scale. The proposed two-step optimization enables to efficiently optimize wind farm layout and thus can be applicable to layout optimization of large-scale wind farms. A case study with the actual Daegwallyeong wind farm shows that wake loss is improved by 2.3% point after the proposed layout optimization which means about 2.5% more energy production compared with the existing layout.

Keywords Wind farms · Optimization · Genetic algorithm · Jensen's model · Daegwallyeong wind farm

1 Introduction

Recently due to the environmental problems caused by existing energy sources and nuclear plant accidents, environmentally friendly energy sources such as wind power, biogas, solar energy, and renewable energy have attracted people's attention, and various optimization studies on wind power [1–10] and solar energy [11, 12] have been proposed to maximize energy generation efficiency at the minimum cost. Among them, a major advantage of the wind power generation is that it does not require any extra cost except repair and maintenance cost. However, since it is very expensive to relocate installed wind turbines, various demonstration tests and optimization studies of wind farm layout have been proposed to maximize its energy generation efficiency. Especially genetic algorithms with various objective functions [13–18] have been widely and successfully used for wind farm layout optimization for energy generation maximization. On the other hand, studies on economic evaluation of relocation of existing batches [19, 20] have been proposed to suggest

relocation decision because already installed wind turbines are not easy to relocate until the design life is reached.

Among the wind farms installed in Korea, the Daegwallyeong wind farm produces the largest amount of wind power, and thus many studies on the farm have been performed [5–9]. Some studies have improved accuracy of the wind analysis model by calibrating weather data using a Weibull distribution [5–7], and there have been researches to find the optimum layout by relocating the existing wind farm layout in a trial and error manner [9]. However, a systematic wind farm layout optimization method has not been yet proposed, and accurate and realistic wind farm analysis models are not considered for the layout optimization.

Consequently, this paper proposes to use the wind farm analysis model considering wake loss implemented in MATLAB for wind farm layout optimization. In addition, two-step layout optimization using a genetic algorithm is proposed for more computationally efficient optimization and is applied to the Daegwallyeong wind farm for a case study. Korea Meteorological Agency's wind data measured in 2017 are utilized in this study.

The remainder of the paper is organized as follows. Section 2 explains the numerical model for wind wake effect considered in the proposed method. Section 3 presents the Daegwallyeong wind farm model to be optimized in this study. Section 4 compares optimized wind farm layout results of the Daegwallyeong wind farm with those from the actual layout. Finally, Sect. 5 concludes the paper.

✉ Ikjin Lee
ikjin.lee@kaist.ac.kr

¹ Korea Advanced Institute of Science and Technology, 291, Daehak-ro, Yuseong-gu, Daejeon, South Korea

² Daejeon Science High School, 46, Gwahak-ro, Yuseong-gu, Daejeon, South Korea

2 Theoretical background

When designing a wind farm, it is important to maximize its economic efficiency or annual production energy by considering various factors such as characteristic of a wind turbine, initial investment, and maintenance cost of the wind turbine as design variables. In the proposed study, all costs including investment and maintenance cost will not be considered during optimization since the number of wind turbines in the Daegwallyeong wind farm will be fixed. Section 2.1 explains the numerical model for wind wake effect and a typical factor for wind turbine installation, Sects. 2.2 and 2.3 describe how to calculate annual energy production and wind speed calibration using the numerical model, respectively, which will be used in the layout optimization explained in Sect. 3.

2.1 Wake effect (vortex phenomenon)

The wake effect phenomenon means that inertia and frictional forces do not flow well in the direction in which air circulates. The flowing fluid rubs against stationary fluid around it where air is vortexed at the interface between the stationary and kinetic fluid. It is a frequent phenomenon when there is a dramatic change in the width of the space through which the fluid can flow. In this paper, the wake effect is considered essential because the weakened wind that passed through the wind turbine reduces energy production efficiency of another wind turbine installed behind. Figure 1 shows wind velocity through the rear wind turbine according to the wake effect of the front wind turbine.

This paper proposes to utilize a numerical model considering the wake effect [1–3] for more accurate wind farm layout optimization. Generally, the amount of energy generated by a wind turbine is determined by the wind speed passing through each wind turbine. To calculate the actual

wind speed of passing through each wind turbine by considering the wind wake effect, Jensen's model is utilized in this study. Considering that, the momentum is preserved in the wake between two wind turbines in Fig. 1, the momentum equilibrium equation can be expressed as

$$\pi r_r^2 v + \pi (r_1^2 - r_r^2) u_0 = \pi r_1^2 u_{ij}, \quad (1)$$

where r_r is the rotor radius, v is the wind speed behind the front rotor, r_1 is the wake radius, u_0 is the oncoming wind speed, and u is the downstream wind speed at a distance x . Then, assuming that the wind speed right behind the rotor is $1/3$ of u_0 [21], the downstream wind speed passing the turbine i under influence of the upstream wind of the turbine j is written as

$$u_{ij} = u_0 \left(1 - \frac{2}{3} \left(\frac{r_r}{r_1} \right)^2 \right). \quad (2)$$

To apply the Jensen model, additional assumption about the turbine rotor radius r_r and distance x is introduced as

$$r_1 = r_r + \alpha x, \quad (3)$$

where entrainment constraint α is defined by

$$\alpha = \frac{0.5}{\ln(z/z_0)}. \quad (4)$$

In Eq. (4), z is the hub height of the wind turbine and z_0 is the surface roughness of ground. In general, the wind speed through the i th wind turbine for n upstream turbines can be written as

$$u_i = u_0 \left(1 - \sqrt{\sum_{j=1}^n \left(1 - \frac{u_{ij}}{u_0} \right)^2} \right). \quad (5)$$

2.2 Annual energy production calculation

Power generation amount of a wind turbine is determined by wind speed and wind turbine type. The wind turbine installed in the Daegwallyeong farm and its power curve will be explained in detail in Sect. 3.2. Once the power generation of a wind turbine for given wind speed is determined, the total annual energy of the wind farm can be calculated as

$$\begin{aligned} AEP_{\text{total}}(\mathbf{X}) &= \sum_{i=1}^{N(\mathbf{X})} AEP_i(\mathbf{X}) \\ &= \sum_{i=1}^{N(\mathbf{X})} \int_0^{360^\circ} \int_0^{u_{\max}} P_i(u_i(u_0, \theta)) \times p(u_0, \theta) \times tdu_0 d\theta, \end{aligned} \quad (6)$$

where \mathbf{X} is a binary design variable vector in grid area, $AEP_{\text{total}}(\mathbf{X})$ is the total annual energy of the farm in MWh,

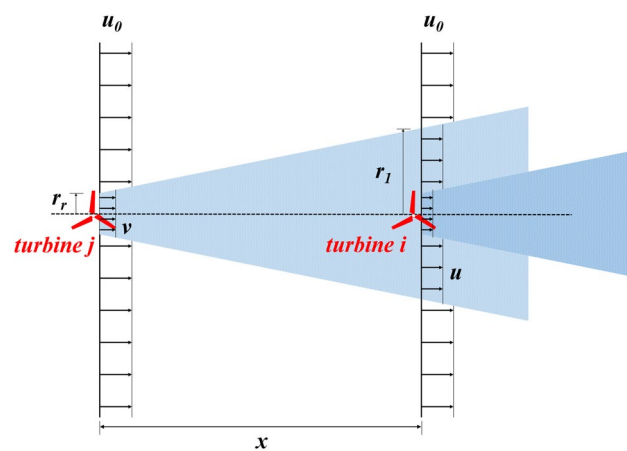


Fig. 1 Schematic of analytical wake effect model

$N(\mathbf{X})$ is the number of the installed wind turbines, $AEP_i(\mathbf{X})$ is the annual energy for the i th turbine in MWh, u_i is the wind speed for the i th turbine considering the wake effect described in Sect. 2.1, θ is the wind direction, and t is the total hours in 1 year, that is, 24×365 . Eq. (6) shows that the multiplication of the power of the i th turbine denoted as $P_i(u_i(u_0, \theta))$ and the probability density function of u_0 and θ denoted as $p(u_0, \theta)$ is integrated to calculate $AEP_i(\mathbf{X})$.

2.3 Site calibration for wind turbine

Since anemometers to measure wind speed are installed in general at lower positions than wind turbines, it is necessary to calibrate the measured wind speed passing through wind turbines. The Deacon equation [22, 23] is utilized for the calibration and expressed as

$$U(z_2) = U(z_1) \left(\frac{z_2}{z_1} \right)^p, \quad (7)$$

where $U(z_1)$ is the wind speed at height of z_1 , and p is the wind rate coefficient defined as

$$p = a + b \ln(U_2), \quad (8)$$

where

$$a = \frac{1}{\ln\left(\frac{z_g}{z_0}\right)} + \frac{0.088}{1 - 0.088 \ln\left(\frac{z_a}{10}\right)}, \quad (9)$$

and

$$b = \frac{-0.088}{1 - 0.088 \ln\left(\frac{z_a}{10}\right)}. \quad (10)$$

In Eqs. (9) and (10), z_g is the geometric altitude mean and z_a is the height of the wind speed measurement. However, since it is difficult to calculate the wind rate coefficient p , data measured at two different heights are substituted into Eq. (7) which yields

$$p = \frac{\ln\left(\frac{U(z_2)}{U(z_1)}\right)}{\ln\left(\frac{z_2}{z_1}\right)}. \quad (11)$$

3 Layout optimization of Daegwallyeong wind farm

3.1 Wind farm model

Currently, 53 wind turbines are installed in the Daegwallyeong wind farm among which 49 wind turbines have been recently installed within a range of 7 km both in horizontal

and vertical directions as shown in Fig. 2. However, due to environmental problems such as roads and mountainous terrain, areas where wind turbines are installable in the above range are limited as marked in red in Fig. 3.

In addition, since the layout optimization of the wind turbines requires a large amount of computations, grids are utilized in the area where the wind turbines are to be installed as in the previous researches. Figure 4 shows the grids created for the limited installable area in Fig. 3. Firstly, 28×28 grids are created in the entire $7 \text{ km} \times 7 \text{ km}$ area which means each grid has a size of $250 \text{ m} \times 250 \text{ m}$. Later, these coarse grids become finer for more accurate layout optimization. Since there are a total of 285 grids in the installable area, layout optimization of the wind farm is performed with 285 binary inputs. Details of the optimization process are discussed in Sect. 3.4.

3.2 Specification of wind turbines

The wind turbines currently installed in the Daegwallyeong wind farm are VESTAS V80 2 MW and generate up to 2 MW energy depending on wind speed passing the wind turbines. Key information of the wind turbines in this study is presented in Table 1. Figure 5 shows the power curve of the wind turbine according to the wind speed. When the wind speed is less than 3 m/s, no energy is generated. On the other hand, when the wind speed is more than 15 m/s, the maximum power is generated as shown in Fig. 5. However, the wind speed higher than 25 m/s is not considered in this study since the wind turbine does not operate at the wind speed due to equipment maintenance problems.

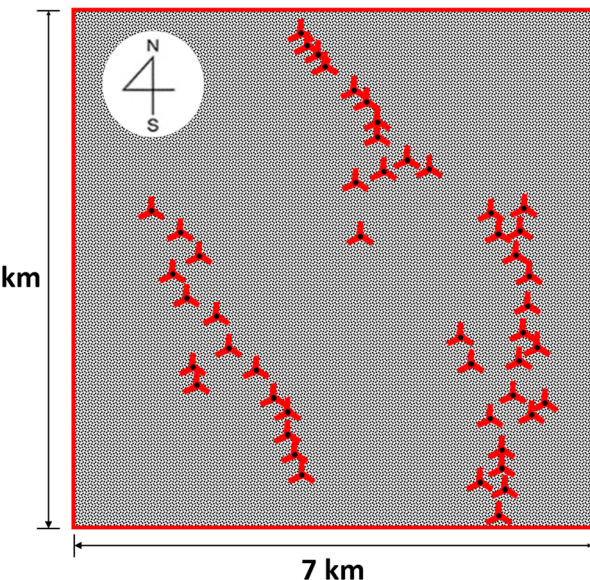


Fig. 2 Wind turbine layout installed in Daegwallyeong wind farm

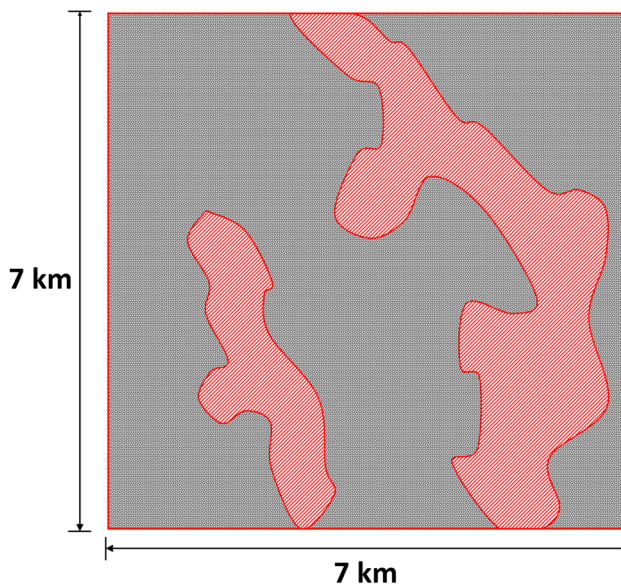


Fig. 3 Limited installable areas in Daegwallyeong wind farm

1	29	57	85	113	141	169	197	225	253	281	309	337	365	393	421	449	477	505	533	561	589	617	645	673	701	729	757
2	30	58	86	114	142	170	198	226	254	282	310	338	366	394	422	450	478	506	534	562	590	618	646	674	702	730	758
3	31	59	87	115	143	171	199	227	255	283	311	339	367	395	423	451	479	507	535	563	591	619	647	675	703	731	759
4	32	60	88	116	144	172	200	228	256	284	312	340	368	396	424	452	480	508	536	564	592	620	648	676	704	732	760
5	33	61	89	117	145	173	201	229	257	285	313	341	369	397	425	453	481	509	537	565	593	621	649	677	705	733	761
6	34	62	90	118	146	174	202	230	258	286	314	342	370	398	426	454	482	510	538	566	594	622	650	678	706	734	762
7	35	63	91	119	147	175	203	231	259	287	315	343	371	399	427	455	483	511	539	567	595	623	651	679	707	735	763
8	36	64	92	120	148	176	204	232	260	288	316	344	372	400	428	456	484	512	540	568	596	624	652	680	708	736	764
9	37	65	93	121	149	177	205	233	261	289	317	345	373	401	429	457	485	513	541	569	597	625	653	681	709	737	765
10	38	66	94	122	150	178	206	234	262	290	318	346	374	402	430	458	486	514	542	570	598	626	654	682	710	738	766
11	39	67	95	123	151	179	207	235	263	291	319	347	375	403	431	459	487	515	543	571	599	627	655	683	711	739	767
12	40	68	96	124	152	180	208	236	264	292	320	348	376	404	432	460	488	516	544	572	600	628	656	684	712	740	768
13	41	69	97	125	153	181	209	237	265	293	321	349	377	405	433	461	489	517	545	573	601	629	657	685	713	741	769
14	42	70	98	126	154	182	210	238	266	294	322	350	378	406	434	462	490	518	546	574	602	630	658	686	714	742	770
15	43	71	99	127	155	183	211	239	267	295	323	351	379	407	435	463	491	519	547	575	603	631	659	687	715	743	771
16	44	72	100	128	156	184	212	240	268	296	324	352	380	408	436	464	492	520	548	576	604	632	660	688	716	744	772
17	45	73	101	129	157	185	213	241	269	297	325	353	381	409	437	465	493	521	549	577	605	633	661	689	717	745	773
18	46	74	102	130	158	186	214	242	270	298	326	354	382	410	438	466	494	522	550	578	606	634	662	690	718	746	774
19	47	75	103	131	159	187	215	243	271	299	327	355	383	411	439	467	495	523	551	579	607	635	663	691	719	747	775
20	48	76	104	132	160	188	216	244	272	300	328	356	384	412	440	468	496	524	552	580	608	636	664	692	720	748	776
21	49	77	105	133	161	189	217	245	273	301	329	357	385	413	441	469	497	525	553	581	609	637	665	693	721	749	777
22	50	78	106	134	162	190	218	246	274	302	330	358	386	414	442	470	498	526	554	582	610	638	666	694	722	750	778
23	51	79	107	135	163	191	219	247	275	303	331	359	387	415	443	471	499	527	555	583	611	639	667	695	723	751	779
24	52	80	108	136	164	192	220	248	276	304	332	360	388	416	444	472	500	528	556	584	612	640	668	696	724	752	780
25	53	81	109	137	165	193	221	249	277	305	333	361	389	417	445	473	501	529	557	585	613	641	669	697	725	753	781
26	54	82	110	138	166	194	222	250	278	306	334	362	390	418	446	474	502	530	558	586	614	642	670	698	726	754	782
27	55	83	111	139	167	195	223	251	279	307	335	363	391	419	447	475	503	531	559	587	615	643	671	699	727	755	783
28	56	84	112	140	168	196	224	252	280	308	336	364	392	420	448	476	504	532	560	588	616	644	672	700	728	756	784

Fig. 4 Grids created for optimization

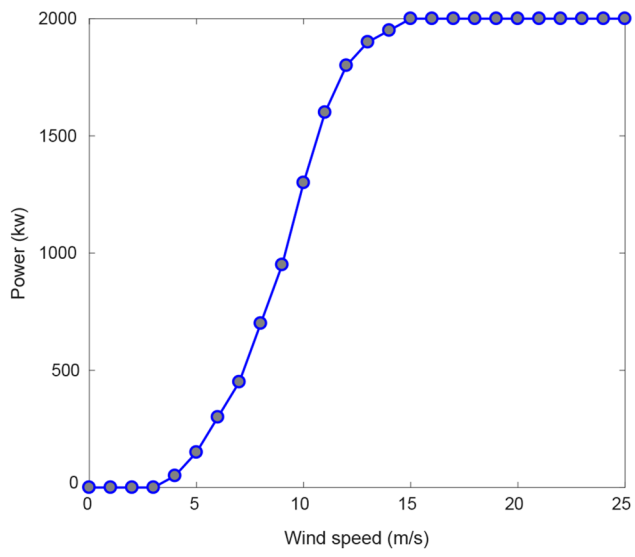


Fig. 5 Power curve of VESTAS V80

3.3 Calibration of wind speed data

In this study, the wind data in the Daegwallyeong area measured every minute from January to December 2017 by Korea Meteorological Agency is utilized [24, 25]. Figure 6 shows the wind speeds measured in an anemometer at a height of 10 m excluding wind speeds less than 3 m/s. As can be seen in Fig. 6, most of wind directions are about 270° which means most of winds blow westward, and most of wind speeds are less than 10 m/s.

Since the height of the wind turbine installed in the Daegwallyeong farm is 80 m, it is necessary to calibrate the measured wind speed according to the height as explained in Sect. 2.3. For the calibration, mean values of the wind speeds measured at specific heights from 2005 to 2009 listed in Table 2 are used. Then, the wind rate coefficient can be estimated as

$$p = \frac{\ln\left(\frac{U(z_2)}{U(z_1)}\right)}{\ln\left(\frac{z_2}{z_1}\right)} = \frac{\ln\left(\frac{5.5}{3.6}\right)}{\ln\left(\frac{80}{10}\right)} = 0.2038. \quad (12)$$

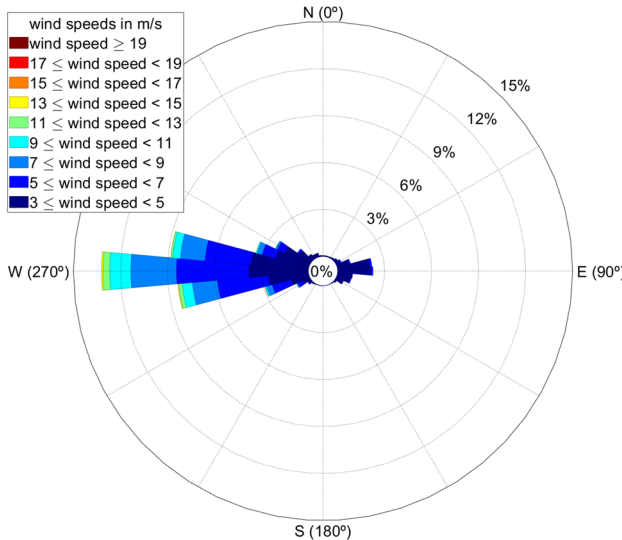
Calibrated wind speeds using Eqs. (7) and (12) are shown in Fig. 7 which shows that the portion of wind speeds above 10 m/s increases significantly after calibration.

3.4 Details for wind farm layout optimization

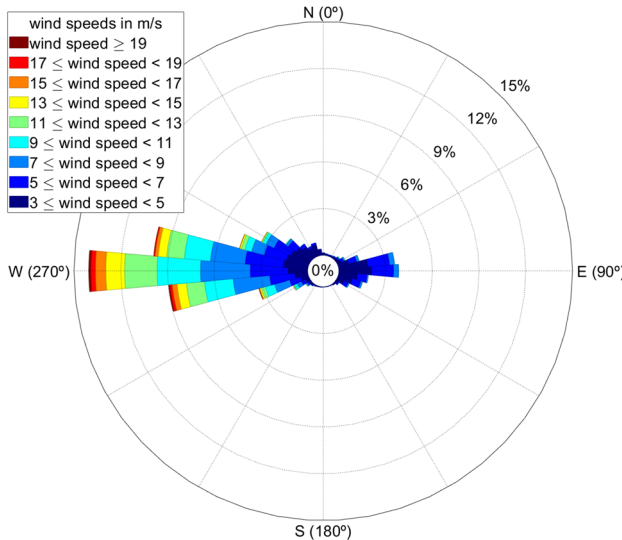
In this study, a genetic algorithm is used for the wind farm layout optimization since it is good at finding a global optimum with discrete or binary inputs. In the proposed study, a batch optimization that yields the maximum energy

Table 1 Specifications of wind turbines

Number of blades	3
Diameter	80 m
Height	80 m
Swept area	5000 m ²

**Fig. 6** Characteristics of wind data measured in 2017**Table 2** Wind speed measured at each height

Height (m)	10	50	80
Wind speed (m/s)	3.6	4.9	5.5

**Fig. 7** Calibrated wind speed data

generation on the grid set shown in Fig. 4 is first performed. Details on the batch optimization are listed in Table 3 which shows that the length of \mathbf{X} is 285, the number of grids in the installable area, and the i th component of \mathbf{X} becomes 1 when a wind turbine is installed in the i th grid otherwise 0. In addition, the objective function is to maximize AEP described in Sect. 2.2, and since the number of wind turbines

Table 3 Information used in the batch optimization

Input variables	Binary input \mathbf{X} of length = 285
Objective function	$\max \text{AEP}_{\text{total}}(\mathbf{X})$
Constraint	$\sum(\mathbf{X}) = 49$

installed in the Daegwallyeong farm is 49, the sum of \mathbf{X} 's components is constrained to be 49.

After the batch optimization, post-optimization is performed to further increase the energy generation. Schematic of the post-optimization is shown in Fig. 8 which shows that the position of a wind turbine is further calibrated within the grid by moving it by half of the grid length. For example, if a wind turbine is installed in the grid 123 as a result of the batch optimization, the wind turbine can be relocated in four positions during the post-optimization. The post-optimization is also performed using the genetic algorithm. Information for the post-optimization is shown in Table 4. The length of \mathbf{X} during the post-optimization is 98 as shown in Table 4 since there are 49 wind turbines and each turbine has two binary coordinate inputs as shown in Fig. 8.

4 Optimization results of wind farm model

To verify the optimized wind farm layout of Daegwallyeong area using the layout optimization and the post-optimization described in Sect. 3.4, we compared annual energy productions obtained from the actual and optimized layouts as shown in Table 5. To see the wake loss effect, annual energy production obtained from the actual layout using no wake model is compared in Table 5 as well. As can be seen in Table 5, annual energy production of the actual wind farm estimated using no wake model is 1.75×10^8 MWh. However, it is 1.55×10^8 MWh using the wake effect model. After the batch optimization, the annual energy production becomes 1.56×10^8 MWh and wake loss is 10.9%. Furthermore, after the post-optimization, the annual energy production is further improved to 1.59×10^8 MWh and the wake loss is 9.1% which is about 2% point less than the batch optimization result.

Figure 9 compares the actual and optimized wind farm layouts, and shows that the number of wind turbines blocking the wind has decreased in the optimized wind farm layout. Figure 10 compares relative wind powers of the actual and optimized wind farms which are the power generated by each turbine divided by the maximum generated power. As can be seen from Fig. 10, the wind power production of the actual wind farm decreases compared with the optimized wind farm. Figure 9 also shows the 39th–49th wind turbines

1	29	57	85	113	141	169	197	225	253	281	309	337	365	393	421	449	477	505	533	561	589	617	645	673	701	729	757
2	30	58	86	114	142	170	198	226	254	282	310	338	366	394	422	450	478	506	534	562	590	618	646	674	702	730	758
3	31	59	87	115	143	171	199	227	255	283	311	339	367	395	423	451	479	507	535	563	591	619	647	675	703	731	759
4	32	60	88	116	144	172	200	228	256	284	312	340	368	396	424	452	480	508	536	564	592	620	648	676	704	732	760
5	33	61	89	117	145	173	201	229	257	285	313	341	369	397	425	453	481	509	537	565	593	621	649	677	705	733	761
6	34	62	90	118	146	174	202	230	258	286	314	342	370	398	426	454	482	510	538	566	594	622	650	678	706	734	762
7	35	63	91	119	147	175	203	231	259	287	315	343	371	399	427	455	483	511	539	567	595	623	651	679	707	735	764
8	36	64	92	120	148	176	204	232	260	288	316	344	372	400	428	456	484	512	540	568	596	624	652	680	708	736	764
9	37	65	93	121	149	177	205	233	261	289	317	345	373	401	429	457	485	513	541	569	597	625	653	681	709	737	765
10	38	66	94	122	150	178	206	235	263	291	319	347	375	403	431	459	487	515	543	571	599	627	655	683	711	739	767
11	39	67	95	123	151	179	207	235	263	291	319	347	375	403	431	459	487	515	543	571	599	627	655	683	711	739	767
12	40	68	96	124	152	180	208	236	264	292	320	348	376	404	432	460	488	516	544	572	600	628	656	684	712	740	768
13	41	69	97	125	153	181	209	237	265	293	321	349	377	405	433	461	489	517	545	573	601	629	657	685	713	741	769
14	42	70	98	126	154	182	210	238	266	294	322	350	378	406	434	462	490	518	546	574	602	630	658	686	714	742	770
15	43	71	99	127	155	183	211	239	267	295	323	351	379	407	435	463	491	519	547	575	603	631	659	687	715	743	771
16	44	72	100	128	156	184	212	240	268	296	324	352	380	408	436	464	492	518	546	574	602	630	658	686	716	744	772
17	45	73	101	129	157	185	213	241	269	297	325	353	381	409	437	465	493	521	549	577	605	633	661	689	717	745	773
18	46	74	102	130	158	186	214	242	270	298	326	354	382	410	438	466	494	522	550	578	606	634	662	690	718	746	774
19	47	75	103	131	159	187	215	243	271	299	327	355	383	411	439	467	495	523	551	579	607	635	663	691	717	747	775
20	48	76	104	132	160	188	216	244	272	300	328	356	384	412	440	468	496	524	552	580	608	636	664	692	720	748	776
21	49	77	105	133	161	189	217	245	273	301	329	357	385	413	441	469	497	525	553	581	609	637	665	693	721	749	777
22	50	78	106	134	162	190	218	246	274	302	330	358	386	414	442	470	498	526	554	582	610	638	666	694	722	750	778
23	51	79	107	135	163	191	219	247	275	303	331	359	387	415	443	471	499	527	555	583	611	639	667	695	722	751	779
24	52	80	108	136	164	192	220	248	276	304	332	360	388	416	444	472	500	528	556	584	612	640	668	696	724	752	780
25	53	81	109	137	165	193	221	249	277	305	333	361	389	417	445	473	501	529	557	585	613	641	669	697	725	753	781
26	54	82	110	138	166	194	222	250	278	306	334	362	390	418	446	474	502	530	558	586	614	642	670	698	726	754	782
27	55	83	111	139	167	195	223	251	279	307	335	363	391	419	447	475	503	531	559	587	615	643	671	699	727	755	783
28	56	84	112	140	168	196	224	252	280	308	336	364	392	420	448	476	504	532	560	588	616	644	672	700	728	756	784

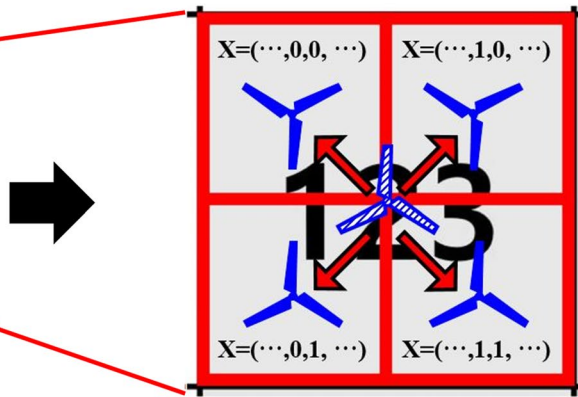


Fig. 8 Schematic of post-optimization

Table 4 Input variables and objective function in the post-optimization

Input variables	Binary input \mathbf{X} of length = 98
Objective function	$\max AEP_{total}(\mathbf{X})$

Table 5 Comparison of annual energy production using wind data measured in 2017

	Annual energy production (MWh)	Wake loss (%)
Actual Daegwallyeong wind farm layout		
No wake model	1.75×10^8	—
Wake model (56 × 56 grids)	1.55×10^8	11.4
Optimized layout (wake model)		
Batch optimization (28 × 28 grids)	1.56×10^8	10.9
Post-optimization (56 × 56 grids)	1.59×10^8	9.1

of the actual wind farm, which show poor energy generation due to the wake loss caused by nearby wind turbines. On the other hand, difference between the maximum and minimum energy generation of wind turbines in the optimized wind farm is relatively small since the wake loss is considered during the optimization.

5 Conclusion

In this study, the wind farm analysis model considering wake loss is applied for layout optimization using a genetic algorithm of the Daegwallyeong wind farm. The actual wind data measured in 2017 in the Daegwallyeong area are used for the layout optimization. For more computationally efficient optimization, two-step layout optimization is proposed where the first step is batch optimization in a large scale and the second step is post-optimization in a small scale. As a result of the Daegwallyeong wind farm layout optimization, the wake loss is reduced by 2.3% point compared with the actual wind farm layout which leads to an additional 0.4×10^7 MWh production per year, that is, about 2.5% more energy production compared with the actual wind farm. This conclusion does not mean that the current layout has to be changed to the layout obtained from the proposed optimization since the Daegwallyeong wind farm is used for verification purpose. However, the proposed method can be applied in the future to the following cases: (1) when economical benefit from relocating wind turbines is higher than relocating cost; (2) when wind turbines in the Daegwallyeong area reach their design life and need to be replaced; (3) when constructing new wind farms not only on land, but also in offshore areas.

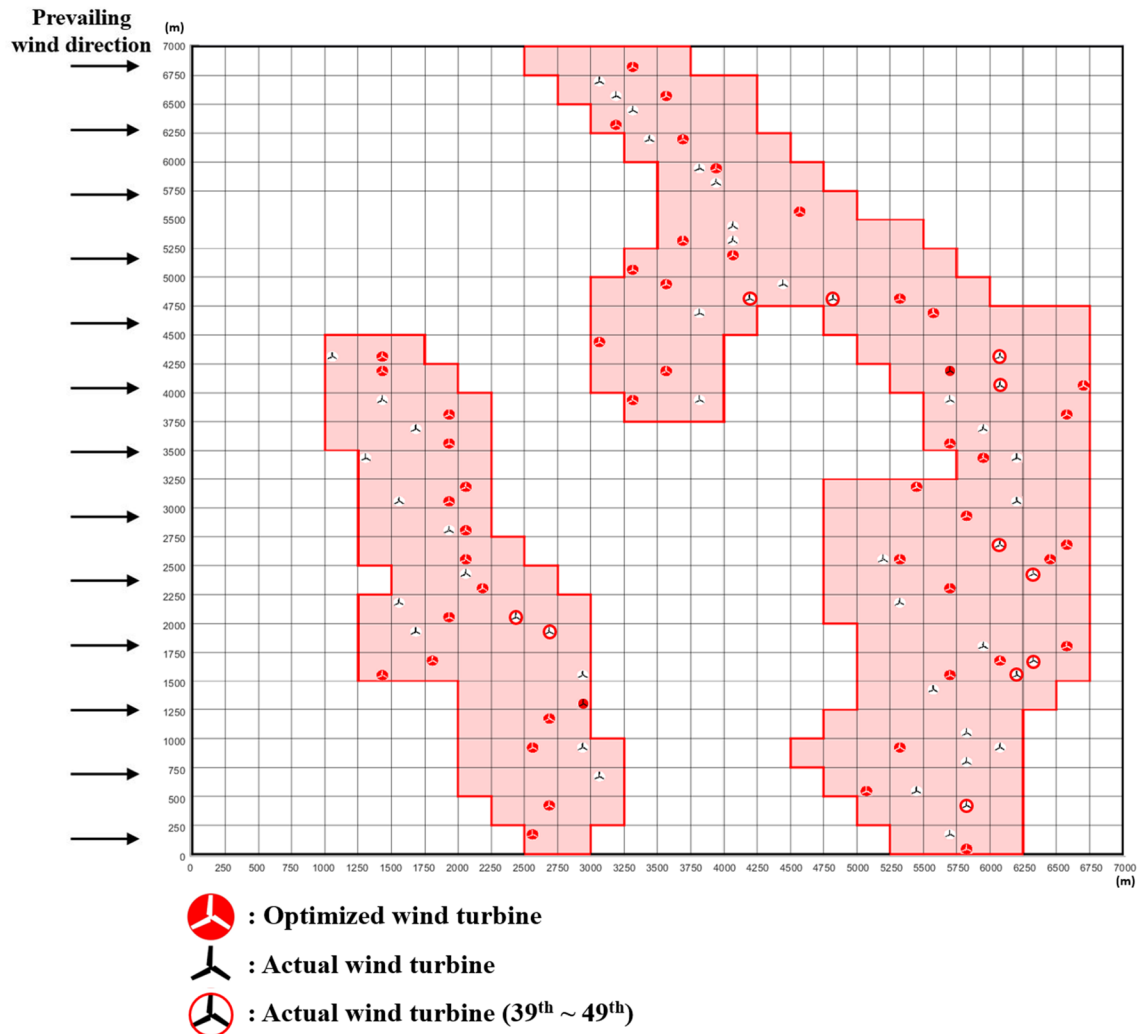


Fig. 9 Comparison of actual and optimized wind farm layouts

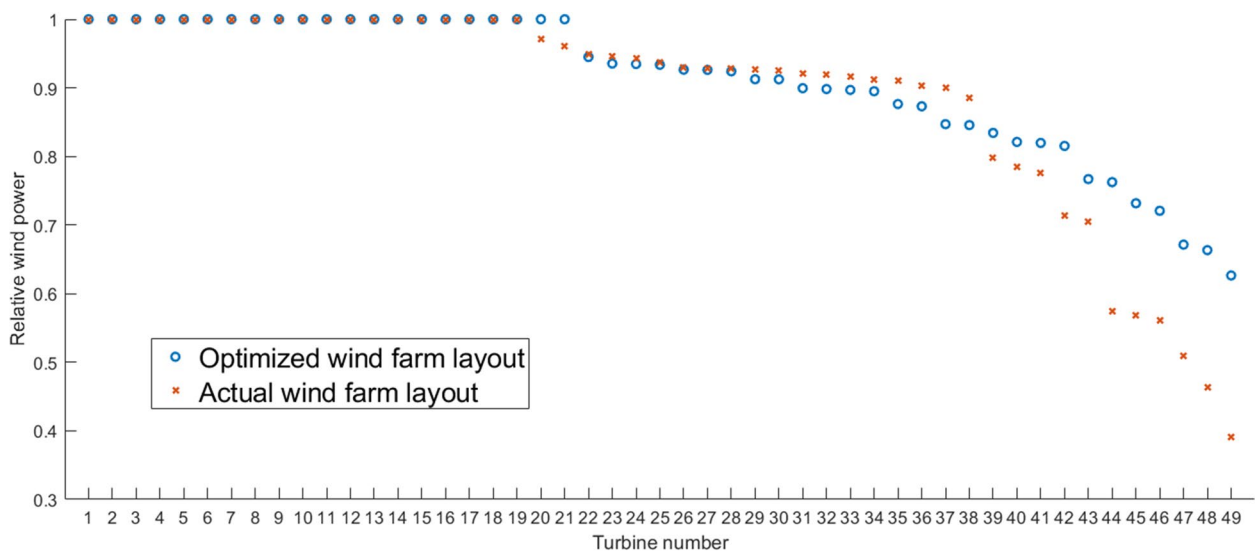


Fig. 10 Comparison of wind power generation between actual and optimized layouts

Acknowledgements This research was supported by Energy Cloud R&D Program through the National Research Foundation of Korea (NRF) funded by the Ministry of Science, ICT (No. 2016006843).

Compliance with ethical standards

Conflict of interest The authors declare that they have no conflict of interest.

References

1. L. Chen, E. MacDonald, A system-level cost-of-energy wind farm layout optimization with landowner modeling. *Energy Convers. Manag.* **77**, 484–494 (2014)
2. B.L. Du Pont, J. Cagan, An extended pattern search approach to wind farm layout optimization. *J. Mech. Des.* **134**(8), 081002 (2012)
3. R. Shakoor, M.Y. Hassan, A. Raheem, Y.K. Wu, Wake effect modeling: a review of wind farm layout optimization using Jensen's model. *Renew. Sustain. Energy Rev.* **58**, 1048–1059 (2016)
4. J. Shin, I. Lee, Reliability-based vehicle safety assessment and design optimization of roadway radius and speed limit in windy environments. *J. Mech. Des.* **136**(8), 081006 (2014)
5. J.W. Ha, S. Kim, A study on the wind power generation and its economic feasibility at Daekwanryung. *J. Energy Eng.* **14**(2), 123–132 (2005)
6. J.K. Woo, H.G. Kim, B.M. Kim, I.S. Paek, N.S. Yoo, Prediction of annual energy production of Gangwon Wind farm using AWS wind data. *J. Korean Sol. Energy Soc.* **31**(2), 72–81 (2011)
7. Y. Nam, N. Yoo, J. Lee, Site calibration for the wind turbine performance evaluation. *KSME Int. J.* **18**(12), 2250–2257 (2004)
8. B.H. Cho, J.W. Lee, Establishment of remote monitoring system for wind turbine test sites based on hierarchical architecture. *J. Korean Soc. Precis. Eng.* **26**(9), 81–87 (2009)
9. M.S. Lee, S.H. Lee, N.K. Hur, A numerical study on the effect of mountainous terrain and turbine arrangement on the performance of wind power generation. *Trans. Korean Soc. Mech. Eng. B* **34**(10), 901–906 (2010)
10. H.G. Kim, Comparative analysis of commercial softwares for wind climate data analysis. *J. Korean Soc. New Renew. Energy* **6**(2), 5–11 (2010)
11. K. Lee, I. Lee, Optimization of a heliostat field site in central receiver systems based on analysis of site slope effect. *Sol. Energy* **193**, 175–183 (2019)
12. S. Kim, I. Lee, B.J. Lee, Development of performance analysis model for central receiver system and its application to pattern-free heliostat layout optimization. *Sol. Energy* **153**, 499–507 (2017)
13. G.P.C.D.B. Mosetti, C. Poloni, B. Diviacco, Optimization of wind turbine positioning in large windfarms by means of a genetic algorithm. *J. Wind Eng. Ind. Aerodyn.* **51**(1), 105–116 (1994)
14. S.A. Grady, M.Y. Hussaini, M.M. Abdullah, Placement of wind turbines using genetic algorithms. *Renew. Energy* **30**(2), 259–270 (2005)
15. J.C. Mora, J.M.C. Barón, J.M.R. Santos, M.B. Payán, An evolutive algorithm for wind farm optimal design. *Neurocomputing* **70**(16–18), 2651–2658 (2007)
16. H.S. Huang, Distributed genetic algorithm for optimization of wind farm annual profits. In 2007 International Conference on Intelligent Systems Applications to Power Systems (pp. 1–6). IEEE (2007)
17. S. Şişbot, Ö. Turgut, M. Tunç, Ü. Çamdalı, Optimal positioning of wind turbines on Gökçeada using multi-objective genetic algorithm. *Wind Energy Int. J. Prog. Appl. Wind Power Convers. Technol.* **13**(4), 297–306 (2010)
18. H.S. Huang, Efficient hybrid distributed genetic algorithms for wind turbine positioning in large wind farms. In 2009 IEEE International Symposium on Industrial Electronics (pp. 2196–2201). IEEE (2009)
19. H.H. Yıldırım, S. Sakarya, Investment evaluation of wind turbine relocation. *Int. J. Optim. Control: Theor. Appl. (IJOCTA)* **9**(3), 6–14 (2019)
20. C.J. Rydh, M. Jonsson, P. Lindahl, Replacement of old wind turbines assessed from energy, environmental and economic perspectives. *Other Inf.* **38**, 1–26 (2004)
21. N.O. Jensen, A note on wind generator interaction. Technical Report Risø-M-2411, Risø National Laboratory (1984)
22. E.H. Cheang, C.J. Moon, M.S. Jeong, K.P. Jo, G.Y. Park, The study for calculating the geometric average height of Deacon equation suitable to the domestic wind correction methodology. *J. Korean Sol. Energy Soc.* **30**(4), 9–14 (2010)
23. E.L. Deacon, P.A. Sheppard, E.K. Webb, Wind profiles over the sea and the drag at the sea surface. *Aust. J. Phys.* **9**(4), 511–541 (1956)
24. Korea Meteorological Agency. “Long-term weather observation”. <https://data.kma.go.kr/data/grnd/selectAsosRltmList.do?pgmNo=36>. Accessed 25 Sep 2019
25. Korea Meteorological Agency. “Observation point data–Sensor/observation elements”. <https://data.kma.go.kr/tmeta/comp/selecCompSenList.do>. Accessed 25 Sep 2019



Jeong Woo Park is a Ph.D candidate of Mechanical Engineering at KAIST, Korea. His current research interests include reliability analysis and design optimization, and multi-fidelity surrogate modeling.



Bo Sung An is a student at Daejeon Science High School, Korea.



Yoon Seung Lee is a student at Daejeon Science High School, Korea.



Ikjin Lee is an Associate Professor of Mechanical Engineering at KAIST, Korea. He received his Ph.D. in mechanical engineering at the University of Iowa. He joined KAIST in 2013. His current research interests include system reliability analysis and design optimization, surrogate modeling, and system robustness analysis and design.



Hyunsuk Jung is a student at Daejeon Science High School, Korea.